9-2015

Phosphorylation State-dependent Interaction Between AKAP7δ/γ and Phospholamban Increases Phospholamban Phosphorylation.

Marc Rigatti
University of Connecticut School of Medicine and Dentistry

Andrew V. Le
University of Connecticut School of Medicine and Dentistry

Claire Gerber
University of Connecticut School of Medicine and Dentistry

Ion I. Moraru
University of Connecticut School of Medicine and Dentistry

Kimberly L. Dodge-Kafka
University of Connecticut School of Medicine and Dentistry

HHS Public Access

Author manuscript

Cell Signal. Author manuscript; available in PMC 2016 March 11.

Published in final edited form as:

Cell Signal. 2015 September ; 27(9): 1807–1815. doi:10.1016/j.cellsig.2015.05.016.

Phosphorylation state-dependent interaction between AKAP7δ/γ and phospholamban increases phospholamban phosphorylation

Marc Rigatti, **Andrew V. Le**, **Claire Gerber**, **Ion I. Moraru**[*], and **Kimberly L. Dodge-Kafka**[*,†]

Pat and Jim Calhoun Center for Cardiovascular Research, UCONN Health, 263 Farmington Ave, Farmington, CT 06030, USA

The Richard D. Berlin Center for Cell Analysis & Modeling, UCONN Health, 400 Farmington Ave, Farmington, CT 06030, USA

Abstract

Changes in heart rate and contractility in response to sympathetic stimulation occur via activation of cAMP dependent protein kinase A (PKA), leading to phosphorylation of numerous substrates that alter Ca^{2+} cycling. Phosphorylation of these substrates is coordinated by A-kinase anchoring proteins (AKAPs), which recruit PKA to specific substrates [1]. Phosphorylation of the PKA substrate phospholamban (PLB) is a critical determinant of Ca^{2+} re-entry into the sarcoplasmic reticulum and is coordinated by AKAP7δ/γ [2,3]. Here, we further these findings by showing that phosphorylation of PLB requires interaction with AKAP7δ/γ and that this interaction occurs only when PLB is unphosphorylated. Additionally, we find that two mutants of PLB (R9C and Δ14), which are associated with dilated cardiomyopathy in humans, prevent association with AKAP7δ/γ and display reduced phosphorylation *in vitro*. This finding implicates the AKAP7δ/γ-PLB interaction in the pathology of the disease phenotype. Further exploration of the AKAP7δ/γ-PLB association demonstrated a phosphorylation state-dependence of the interaction. Computational modeling revealed that this mode of interaction allows for small amounts of AKAP and PKA (100–200nM) to regulate the phosphorylation of large quantities of PLB (50μM). Our results confirm that AKAP7γ/δ binding to PLB is important for phosphorylation of PLB, and describe a novel phosphorylation state-dependent binding mechanism that explains how phosphorylation of highly abundant PKA substrates can be regulated by AKAPs present at ~100–200 fold lower concentrations.

Keywords

AKAP; Phosphorylation; Anchoring; Scaffold; phospholamban

[†]Address for Correspondence: Kimberly L. Dodge-Kafka, Pat and Jim Calhoun Center for Cardiovascular Research, University of Connecticut Health Center, MC3946, EG028, 263 Farmington Ave, Farmington, CT 06030, dodge@uchc.edu, Phone: (860) 679-2452, Fax: (860) 679-1426.

[*]co-corresponding authors

Author Contributions

M.R. designed and analyzed the computational model and wrote the manuscript. A.V.L. performed the Biacore experiments and analyzed data. C.G. performed the in vitro kinase assays. I.I.M analyzed the computational models and experimental data. K.D.K. conceived of the study, designed and performed experiments, analyzed data, and wrote the manuscript.

1 Introduction

The heart responds to an increase in sympathetic stimulation via activation of the cAMP-dependent protein kinase PKA, leading to phosphorylation of several key substrates. These substrates mediate Ca^{2+} entry, release, and uptake into intracellular stores. Phosphorylation therefore allows the heart to increase the force contraction and the rate of relaxation by changing the kinetics of the Ca^{2+} transients that underlie these physiological events. Importantly, several key studies have demonstrated that PKA must be compartmentalized with its substrate in the heart in order for phosphorylation to occur [4]. This is accomplished via A-kinase anchoring proteins (AKAPs), a class of scaffolding proteins that compartmentalize PKA with its substrates, thereby forming a microdomain of PKA activity. Importantly, disruption of PKA anchoring using global AKAP/PKA disrupting peptides greatly impacted the contractile response of the myocyte to sympathetic stimulation, demonstrating the importance of AKAPs for regulation of cardiac Ca^{2+} dynamics [5,6].

A key AKAP that plays a role in the regulation of cardiac Ca^{2+} dynamics is AKAP7 [7]. This AKAP has four splice variants (α, β, γ and δ), which display a range of molecular weights from 18 to 50 kDa [8]. AKAP7δ/γ plays an important role in the rate of relaxation of the heart via mediating the phosphorylation of the cardiac protein phospholamban (PLB) [3]. In its unphosphorylated state, PLB binds to the Sarcoplasmic Reticulum Ca^{2+}-ATPase (SERCA2) pump and decreases pump action, thus providing a rate-limiting step in the cardiac contraction/relaxation cycle. In contrast, phosphorylation of PLB disrupts the PLB/SERCA2 interaction, thereby accelerating Ca^{2+} re-uptake into cardiac stores and allowing for an increase in the rate of relaxation. Importantly, peptide-based disruption of the AKAP7δ/PLB interaction in the rat myocyte significantly attenuated the sympathetic-promoted phosphorylation of the protein and the increase in Ca^{2+} re-uptake associated with stimulation [3]. It is important to note that AKAP7δ is replaced by AKAP7γ in the human and mouse myocyte [9]. Hence, it has been suggested that this interaction could be used as a potential drug target in heart failure patients [10].

A number of AKAP7δ/γ binding partners with the capacity to influence PLB phosphorylation have been identified including protein kinase C (PKC), protein phosphatase-1, inhibitor-1 (I-1), and phosphodiesterase 3A (PDE3A) [11–13]. This evidence provides us with the key elements of the AKAP7δ/γ signaling microdomain, which may control PLB phosphorylation. However, one particularly critical question exists: how does a low abundance protein like AKAP7δ/γ regulate phosphorylation of a very high abundance protein like PLB? This question was eloquently posed by Don Bers in his 2002 review of cardiac-excitation contraction coupling, commenting "…*it is less clear how targeting would practically work for phospholamban and troponin I phosphorylation (as compared with* I_{Ca} *or Ryanodine Receptor). This would require very high amounts of the various anchoring and signaling proteins because troponin I and phospholamban are present at 50μM or higher concentrations and are dispersed widely in the cell* [14]."

The implied assumption of AKAP microdomain signaling is that AKAPs remain bound to their respective PKA substrates regardless of the state of the complex. If true, such a mechanism would require an abundance of both AKAP and its binding partners that is

similar to that of the PKA substrates – but the cellular concentration of PKA is not nearly as high as PLB, nor are the concentrations of AKAP7δ/γ or its other binding partners (Protein phosphatase 1, Inhibitor-1 and Phosphodiesterase 3A) [12,15–18]. However, it is clear that the AKAP plays an important role in the phosphorylation of PLB [19]. Here, we confirm that binding of PKA to AKAP7δ/γ is required for PLB phosphorylation and that deletion of the PKA binding domain on the AKAP7 results in a significant reduction in PLB phosphorylation. Importantly, several human mutants of PLB, which are known to exhibit decreased phosphorylation and are associated with dilated cardiomyopathy, do not interact with AKAP7δ/γ, further suggesting that the PLB/AKAP7δ/γ is necessary for phosphorylation. Therefore, the question remains: how are these AKAP-binding requirements compatible with the efficient phosphorylation of large amounts of PLB? We hypothesized that this could be explained by our newly observed phosphorylation state-dependent binding of AKAP7δ/γ to PLB. Here, we show that the high affinity association between AKAP7δ/γ and PLB is lost upon phosphorylation of PLB. A computation model of the detailed biochemical kinetics of the pathway showed that if state-dependent binding is included in the reaction network, phosphorylation of high concentrations of PLB is possible at low concentrations of both AKAP7γ and PKA, consistent with the observed results [19]. Importantly, our experimental findings and kinetic analysis provide a mechanistic hypothesis of AKAP7δ/γ complex signaling in cardiac myocytes that reconciles the problem with disparity of complex component concentrations.

2 Experimental Methods

2.1 Antibodies

The following primary antibodies were used for immunoblotting: mouse monoclonal Phospholamban (Millipore; 1:1000 dilution), polyclonal phosphor-phospholaman serine 16 (Millipore; 1:500), mouse monoclonal GFP (Santa Cruz Biotechnology; 1:500 dilution), polyclonal mCherry (Thermo Scientific Pierce; 1:3000 dilution), monoclonal PKA RIIα subunit (Santa Cruz Biotechnology; 1:500).

Immunoprecipitations were carried out using the following antibodies: polyclonal AKAP7 (Sigma; 5 μg), mouse monoclonal GFP (Santa Cruz Biotechnology; 5 μg), mouse monoclonal Phospholamban (Millipore; 3 μg)

2.2 Expression constructs

The human phospholamban construct was obtained Origene and amended with EcoRI/BamHI restriction sites using PCR, and subcloned into the peGFP-N1 vector. Mutant phospholamban constructions were made by site directed mutagenesis.

2.3 Cell Transfection and Immunoprecipitation

HEK293 cells were transfected at 50–70% confluency in 60 mm plates using the calcium phosphate method with 6 μg of each plasmid DNA. Cells were treated with various drugs for the time given, and cell lysate was collected in 0.5 ml HSE buffer (HEPES, pH 7.4, 150 mM NaCl, 5 mM EDTA, 1% Triton X-100 and protease inhibitors). Supernatants were incubated overnight at 4°C with the indicated antibody and 15 μl of prewashed protein A-or G-agarose.

Following extensive washing, captured proteins were solubilized in 2X sample buffer and analyzed by immunoblot.

Rat heart extract was prepared as previously described [20,21]. Immunoprecipitating antibodies were added to 500 μl of extract along with 13 μl protein agarose. After an overnight incubation followed by extensive washing, captured proteins were analyzed by immunoblot.

2.4 In vitro Phospholamban phosphorylation assays

Various PLB peptides (1 μg) were incubated in kinase buffer (50 mM Tris-HCL pH 7.5, 5 mM $MgCl_2$) containing 100 μM ATP, 5 μM [γ^{-32}]ATP and 800 units of purified PKA catalytic subunit (NEB). After a 15 minute incubation at 30°C, the reaction mixture was spotted onto phosphocellulose strips and washed five times in 75 mM phosphoric acid. Filters were air dried and counted.

2.5 Rat neonatal myocyte culture

Myocytes were prepared from 2 day old Sprague-Dawley rats, as previously described. Cell were plated in Dulbecco's Modified Eagle medium (DMEM)with 17% Media 199, 1% penicillin/streptomycin solution, 10% horse serum and 5% fetal bovine serum (FBS) at 125,ooo per cm2. After an overnight incubation in plating medium, the myocytes were maintained in culture for up to one week in maintenance medium (79%DMEM, 20% Media 199, and antibiotic). Cells were stimulated with the various drugs as described.

2.6 Surface Plasmon Resonance

SPR analysis was performed using a BIAcore T100. Biotinylated-Phospholamban peptide (Chi Scientific) was covalently immobilized using NHS (N-hydroxysuccinamide) and EDC [1-ethyl-3-(3-(dimethylamino)propyl)carbodiimide] (Biacore amine coupling kit) to the surface of a sensor chip (BIAcore type CM5). The amount of ligand bound (in resonance units, RUs) was 300 RU. AKAP7γ protein analyte was diluted at increasing concentrations (12.50–200 nM) in HBS buffer (10 mM HEPES (pH 7.4), 150 mM NaCl, and 0.005% Surfactant P20) and injected over the sensor surface at a flow rate of 30 μL/min for 300 seconds. Post injection phase, dissociation was monitored in HBS buffer for 300 seconds at the same flow rate. The surface was regenerated between injections using 10 mM NaCl at a flow rate of 50 μL/min for 30 seconds. Sensorgrams were all processed by BIAcore T100 evaluation software.

2.7 GST-RII pulldown assay

Beads charged with RIIα-GST fusion protein were incubated with isolated cell lysate transfected as described above. After an overnight incubation at 4C with shaking, beads were washed extensively and captured proteins were solubilized in 2X sample buffer and analyzed by immunoblot.

2.8 Computational Modeling of the AKAP7/Phospholamban complex

An ordinary differential equation (ODE) model of PLB phosphorylation by AKAP7δ/γ bound PKA was implemented using the Virtual Cell modeling software. The reaction

network is composed two basic modules; 1) cAMP production and PKA activation and 2) AKAP7δ/γ binding and phosphorylation of PLB with a total of 18 species and 14 reactions (Table 1, Fig S1). Activation of AC via association with Gs in module 1 results in the production of cAMP that binds PKA (R2C2) resulting in sequential dissociation of each of two catalytic subunits (C). Free C is able to phosphorylate Gs within the GsAc complex resulting in the inhibition of cAMP production and, in conjunction with the activity of PDE, the return of cAMP levels to baseline. Due to the high affinity interaction of cAMP with the PKA regulatory subunit (R), C does not reassociate with R to form PKA (R2C2) following cAMP stimulation. In order to return PKA activity to baseline following stimulation we allowed cAMP bound R (R2_cAMP) to be stripped of cAMP by PDE (reference). In the second module of the reaction network PLB associates with AKAP to form a complex (AKAP_PLB) followed by phosphorylation of PLB (AKAP_pPLB). All AKAP is bound to PKA derived from the total pool of PKA in module 1. Since AKAP bound PKA activity represents only a fraction of the total PKA activity, the total AKAP-PKA activity is defined by the following equation:

$$[E] = 2 * AKAP\_PLB * \left(\frac{C}{2 * R2C2 + R2C1 + C} \right)$$

where E represents the total amount of enzyme (active PKA) from the AKAP bound pool of PKA that is available to participate in the phosphorylation of PLB which, is defined by standard Michaelis-Menten kinetics:

$$[pPLB] = \frac{[E] * k_{cat} * [AKAP\_PLB]}{(Km + [AKAP\_PLB])}$$

To simulate the difference between phosphorylation state-dependent (AKAP does not bind pPLB) and phosphorylation state-independent (AKAP binds both PLB and pPLB) the reverse rate for the interaction of AKAP and pPLB was modulated so that AKAP bound pPLB with either equal or lower affinity than PLB.

For state-independent binding, the affinity of AKAP for pPLB is the same as in the non-phosphorylated state and for state-dependent binding the forward rate was increased. For state-dependent binding to PLB the reverse rate of the AKAP-pPLB interaction was increased by a factor of 1000, changing the affinity from 13.3nm to 13.3μM. The model is available in the public biomodels folder of the Virtual Cell software.

3 Results

3.1 AKAP7γ directly binds to phospholamban

Due to conflicting evidence demonstrating the importance of AKAP7δ/γ for phospholamban (PLB) phosphorylation [3,19], we investigated the dynamics of AKAP7 binding to PLB as a possible regulatory function of phosphorylation. To begin with, we confirmed previous findings that AKAP7δ/γ binds directly to PLB [3]. As shown in Figure 1A, PLB co-immunoprecipitated with AKAP7 from isolated rat heart extract, but not with control IgG,

demonstrating that these two proteins form a complex in cardiac myocytes. Next, we investigated if this interaction was specific for the cardiac myocyte, or if association could be detected in a heterologous system. HEK293 cells were transfected with plasmids expressing mCherry-AKAP7γ in the presence and absence of GFP-phospholabman. GFP was immunoprecipitated and the association of AKAP7γ was determined by Western blot analysis (Figure 1B). Importantly, co-precipitation of mCherry-AKAP7γ was only seen in cells expressing GFP-PLB, demonstrating the specificity of the interaction. To further these findings and examine the kinetic properties of the interaction, we performed surface plasmon resonance (SPR). As the domain on phosholamban for binding to AKAP7 is maintained in the first 21 amino acids, we immobilized a peptide mimicking this domain on a CM5 sensor chip. Varying concentrations of purified AKAP7γ were used to determine the dynamics of the interaction. As shown in Figure 1C, we confirmed a direct interaction between phospholamban and AKAP7γ with an affinity of 13.3nM. Analysis of the fit of the interaction suggests one site of interaction. Taken together, these data confirm the original observation demonstrating a direct association of AKAP7 with phospholamban that can be isolated from cardiac myocytes.

3.2 PKA bound to AKAP7δ/γ is responsible for phosphorylation of phospholamban

The primary purpose of AKAPs is to co-localize PKA and its substrate via formation of a multi-component signaling complex, resulting in enhanced substrate phosphorylation. Therefore, we next examined the necessity of PKA binding to AKAP7δ/γ for PLB phosphorylation. To investigate this association in an endogenous tissue, PLB was immunoprecipitated from rat heart lysate, and association with PKA was determined in the presence or absence of the AKAP/PKA disrupting peptide AKAP-IS (Figure 2A) [22]. Disruption of PKA anchoring using the AKAP-IS peptide decreased association of the PKA RII subunit with PLB. Importantly, incubation of a control peptide did not significantly affect PKA/PLB interaction, demonstrating that PKA associates with PLB via interaction with AKAP. To determine the role of AKAP7γ in mediating this association, HEK293 cells were transfected with GFP-PLB and either wild-type mCherry-AKAP7γ, or one lacking the PKA binding domain (mCherry-ΔPKA-AKAP7γ). Lysate isolated from these cells was subjected to pulldown analysis using GST-tagged PKA RIIα subunit. This is a common technique used to isolate AKAP complexes from various tissues, as the RII subunit will pulldown the AKAP and all AKAP-associated proteins [12,23]. As shown in Figure 2B, GFP-PLB only associated with the PKA subunit in the presence of full-length AKAP7γ. However, when the PKA binding domain was deleted from the AKAP, GST-RIIα could no longer pulldown PLB, demonstrating the importance of PKA anchoring to AKAP7γ. Taken together, these results implicate AKAP7γ for linking the kinase to the PLB complex.

Next, we investigated the functional significance of this interaction for regulation of PLB phosphorylation. We first performed analogous experiments to those outlined in Figure 2B, and looked at the role of AKAP7γ-bound PKA on PLB phosphorylation. As shown in Figure 2C, expression of the anchoring protein dramatically heightened PLB phosphorylation. However, when the PKA binding domain was deleted from the AKAP, this enhancement was lost, suggesting that the kinase must be attached to the AKAP for this effect.

3.3 Described human mutations of phospholamban contained in the AKAP7δ/γ binding domain decrease complex formation, thereby reducing phosphorylation

Multiple mutations of PLB have been identified and linked to familial dilated cardiomyopathy. At least two of these mutations are found in the AKAP7δ/γ binding domain, suggesting these mutation may affect the ability of PLB to bind to the AKAP (Schematic diagram shown in Fig 3A). First, mutation of Arginine 9 to Cystine (PLB-R9C) displayed a dose-dependent inhibition of SERCA2a and significantly decreased phospho-PLB [24]. The other is deletion of Arginine 14 (PLB-Δ14). This mutation exhibited super-inhibition of SERCA2a activity, correlating with decreased PLB phosphorylation [25]. To test the importance of AKAP7δ/γ binding to PLB for the phosphorylation of PLB, we utilized these mutations to block the association. To begin, we examine the strength of interaction between AKAP7γ and these mutations using surface plasmon resonance (SPR). Peptides mimicking the first 21 amino acids of wild-type PLB, or ones containing the defined mutations (PLB-R9C and PLB-Δ14) were immobilized on a CM5 sensor chip, and the changes in the kinetic strength of the interaction was determined using varying concentrations of purified AKAP7γ flown over the chip. As shown in Figure 3B, these mutations dramatically affected the ability of the AKAP to bind to PLB, as the affinity of these two mutants for AKAP7γ are below the limit of detection.

Our SPR data suggest that mutation of the AKAP7δ/γ binding domain on PLB reduces the interaction with the AKAP. We therefore investigated if these mutations affected the ability of the complex to form in a cellular environment. AKAP7γ was coexpressed in HEK293 with wild-type PLB-GFP, or one of the mutated isoforms (PLB-R9C-GFP or PLB-Δ14-GFP). The PLB-GFP complex was isolated and association of AKAP7γ-mCherry was determined by Western Blot. As shown in Figure 3C, both mutations significantly decreased the co-precipitation of AKAP7γ, suggesting that a decrease in the AKAP7γ binding affinity measured in these mutants results in decreased association of AKAP7 with the protein in a cellular context.

Importantly, the decrease in complex formation seen with the PLB mutants should reduce the concentration of PKA found in the PLB complex. To test this hypothesis, AKAP7γ was coexpressed in HEK293 with wild-type PLB-GFP, or one of the mutated isoforms (PLB-R9C-GFP or PLB-Δ14-GFP). Cell lysate was subjected to GST-RII pulldown, and association of GFP-PLB was measured. In confirmation of our findings, wild-type PLB associates with the PKA subunit when co-expressed with AKAP7γ (Figure 3D). However, both PLB mutations showed decreased association with the GST-RII, suggesting mutation of PLB in the AKAP7δ/γ binding domain decreases complex formation and reduces PKA association with PLB.

As our hypothesis states that AKAP7δ/γ anchored PKA mediates the phosphorylation of PLB, the decrease in complex formation seen with the mutated isoforms of PLB should therefore result in a decrease in phosphorylation of the protein. To test this hypothesis, AKAP7γ was coexpressed in HEK293 with wild-type PLB-GFP, or one of the mutated isoforms (PLB-R9C-GFP or PLB-Δ14-GFP). Cells were stimulated with 100 nM Isoproterenol for 5 minutes, and phosphorylation of PLB was determined by Western Blot analysis (Figure 3E). In collaboration with those results seen in both transgenic and human

patients [24,25], less phosphorylation was seen with the mutated isoforms of PLB. This finding correlates with the decreased PKA association within the mutant complexes due to deceased affinities for AKAP7, suggesting that one mechanism for the attenuation of phosphorylation of the mutant PLB isoforms is a significant decrease in the localization of the kinase to the complex. However, it is plausible that this effect may result from a decreased ability of these mutated isoforms to be phosphorylated by the kinase and not a disruption in the localization of the kinase to the PLB complex. To test this, peptides mimicking the first 21 amino acids of wild-type PLB, PLB-R9C or PLB-Δ14 were subjected to an *in vitro* kinase assay. As shown in Figure 3F, all peptides were able to be phosphorylated by the kinase to a similar extent, suggesting the decrease in phosphorylation of the mutated PLB isoforms seen in the exogenous system is not due to a lack of ability of the kinase to phosphorylate the mutated isoforms. Taken together, the data shown in Figure 3 supports the hypothesis that by linking the kinase to its substrate PLB, AKAP7δ/γ mediates phosphorylation of PLB.

3.4 Phosphorylation of phospholamban decreases the affinity for AKAP7δ/γ binding

Contained in the AKAP7δ/γ binding domain on PLB is the PKA phosphorylation site. We therefore proposed that phosphorylation of PLB would decrease the ability of the AKAP to interact with the protein. To test this hypothesis, we began by defining the change in affinity between phosphorylated PLB and non-phosphorylated PLB using SPR. We immobilized a peptide mimicking the first 21 amino acids of either wild-type PLB, or one that is permanently phosphorylated at Serine 16 to a CM5 sensor chip, and then determined the kinetic strength of the two interactions using varying concentrations of purified AKAP7γ. As shown in Figure 4A, when phosphorylated, the affinity of AKAP7γ and PLB is below the limit of detection, suggesting a low affinity binding. To confirm this finding in a cellular context, HEK293 cells were transfected with plasmids expressing mCherry-AKAP7γ and GFP-PLB. After a 15 minute stimulation with 100 nM Isoproterenol, GFP was immunoprecipitated and the association of AKAP7γ was determined by Western blot analysis (Figure 4B). Importantly, co-precipitation of mCherry-AKAP7γ was dramatically decreased under conditions that result in phosphorylation of PLB. These findings were confirmed in an endogenous setting. Rat neonatal myocytes were stimulated with 10 μM Isoproterenol for 15 minutes. Phospholamban was immunoprecipitated and association with the AKAP was determined by Western Blot. Taken together, these findings suggest that the AKAP7δ/γ interaction with PLB is dispersed upon activation of PKA and phosphorylation of PLB.

3.5 Phosphorylation state specific binding of AKAP7δ/γ increases phospholamban phosphorylation

Our finding that the AKAP7δ/γ-PLB interaction is phosphorylation state specific is interesting given that the purpose of this interaction is to direct PKA phosphorylation to PLB. Such state selective binding suggests that AKAP7δ/γ likely binds, phosphorylates, and then unbinds PLB in a dynamic process with the potential to increase PLB phosphorylation in comparison to remaining bound regardless of phosphorylation state.

To investigate the potential consequence of state selective binding of AKAP7δ/γ to PLB, we created an ordinary differential equation model that simulates phosphorylation of PLB by AKAP7δ/γ bound PKA at baseline steady state and during cAMP stimulation. For all iterations of the model parameters, the simulation was run for 15000s prior to initiating our stimulation protocol, thus ensuring that all species reach a baseline steady state. At baseline steady state, the level of cAMP is 244nm and 2.4% of the total PKA is in an active state. Following initiation of our stimulation protocol, the levels of cAMP rise to 5.6μM activating 94.1% of the total PKA in 90s and decaying back to baseline in roughly 500–600s (Figure 5A). To test the effect of state specific binding, we compared the levels of phospho-PLB with either equal affinity of AKAP for PLB and phospho-PLB (state-independent), or 1000-fold lower affinity for pPLB (state-dependent). We tested AKAP concentrations ranging from 1–250nM for both state-independent binding and state-dependent binding. Unpublished analysis from our lab and others suggest that the level of AKAP7δ/γ present in cardiac myocytes is roughly 100nm. The total amount of PLB present in these simulations is 50μM [14]. In the range of AKAP concentrations tested, state-independent binding of AKAP to PLB provides minimal capacity for PLB phosphorylation, with very low levels of phosphorylation at baseline and minimal response to stimulation (Figure 5B). We quantified the response to stimulation by calculating the dynamic range, defined as the change in concentration of phospho-PLB from baseline to maximum, divided by the total concentration of PLB. The dynamic range for state-independent binding ranges from 0.01% to 0.17% (Figure 5C). State-dependent binding of AKAP to PLB however, allows for maintenance of low baseline levels of PLB phosphorylation and dramatic responses to stimulation (Figure 5B). With state-dependent binding, the dynamic range varies from 0.05% to 42.3% (Figure 5D). It is important to note that while the primary determinants of the dynamic range of PLB phosphorylation are the affinity of AKAP for phospho-PLB and the AKAP concentration, the dynamic range is also modified significantly by baseline cAMP concentration and the amount of phosphatase present in the system. Higher baseline levels of cAMP (622nm) contribute to increased baseline activity of PKA and hence higher levels of phospho-PLB (Figures 6A and 6B). With the same level of stimulation, this results in a decreased dynamic range (Figure 6C). Additionally, it was noted that at higher baseline cAMP levels, increasing the AKAP concentration past 0.15μM resulted in dramatic increases in baseline phospho-PLB. While this threshold effect of AKAP concentration on baseline phospho-PLB will occur in the simulations with lower baseline cAMP levels, it requires higher concentrations AKAP than we would expect to see *in vivo*. We determined that this is primarily due to a shift in the balance of PKA and phosphatase activity. Increasing the amount of phosphatase in the simulations allowed for maintenance of lower baseline phospho-PLB levels for AKAP concentrations at the top of our range, and slightly reduced maximal phospho-PLB for all AKAP concentrations. This resulted in a reduced dynamic range at lower AKAP concentrations, yet increased the dynamic range at higher AKAP concentrations in comparison to simulations with a lower phosphatase concentration (Figure 6D). The model demonstrates that phosphorylation state-dependent binding of AKAP7δ/γ to PLB could allow low concentrations of AKAP7γ to phosphorylate much higher concentrations of PLB. Additionally, the data suggests that the significant increase in dynamic range seen with state-dependent binding is stable over a range of baseline cAMP

and phosphatase concentrations, perhaps allowing for fine-tuning of AKAP7γ complex signaling.

4 Discussion

The importance of AKAP7δ/γ to PLB phosphorylation and cardiac calcium dynamics has recently been called into question by the work of Jones *et al* [19]. Their AKAP7 PKA binding domain knockout mouse displayed no obvious phenotype, nor any defect in PLB phosphorylation or Ca^{2+} handling in response to sympathetic stimulation. Hence, the authors suggest that AKAP7 is not responsible for anchoring PKA to PLB, and suggest that another AKAP likely performs this function. Their deletion construct is expected to ablate only the PKA and $Ca_v1.2$ binding domains of all AKAP7 isoforms, although no effect on L-type calcium current were seen. It is concerning that the authors did not demonstrate that the truncated protein products to not associate with PKA. Additionally, it is noteworthy that previous work by this group found that complete ablation of AKAP5 in mice does not show an obvious phenotype, while specific ablation of the PKA binding domain does [26]. It is possible that deletion of exon 7 behaves more like a full length AKAP7-knockout, which is consistent with the lack of detection of all isoforms of the AKAP in this model. Additionally, if a truncated version of AKAP7δ/γ is still expressed in the mouse, it would still bind all the other components of the complex and perhaps the balance of phosphorylation to dephosphorylation is changed. Further investigation of this mouse model is warranted before concluding that AKAP7δ/γ anchoring to PKA is not important.

However, the data shown here clearly demonstrates the role of AKAP7δ/γ in mediating phosphorylation of PLB. AKAP7δ/γ was first identified as the AKAP that directs PKA mediated phosphorylation of PLB by Lygren *et al* in 2007. This work showed that disruption of the AKAP7δ-PKA interaction results in a reduction in PLB phosphorylation by approximately 50% and that this has a significant effect on Ca^{2+} dynamics [3]. Our work confirms this finding by showing that disruption of PKA binding to the complex, or decreasing the affinity for AKAP7 and PLB reduces PKA phosphorylation of PLB. Hence, AKAP7δ/γ should be a key player in the calcium dynamics of the heart.

Several human PLB mutations have been discovered which are associated with dilated cardiomyopathy. Two PLB mutants in particular, PLB-R9C and PLB-Δ14, display hypo-phosphorylation, yet the mechanism of the decrease in phosphorylation is unclear at present [24,25]. We examined the ability of these PLB mutants to associate with AKAP7γ and found a significant reduction in binding affinity compared to WT PLB that correlated with a decrease in PKA association with the complex and a reduction in phosphorylation of the mutant proteins when compared to wild-type PLB. Together, these findings suggest that the impaired interaction of these PLB mutants with AKAP7δ/γ may contribute to their hypo-phosphorylation. Given the clinically significant phenotype associated with these mutants, our findings indicate that the AKAP7δ/γ-PLB interaction is critically important for maintaining PLB phosphorylation and normal cardiac function in humans.

Phosphorylation of PLB by PKA occurs at Serine 16, which is located within the region of the AKAP7δ/γ binding site. The location of this phosphorylation site suggests that it may

affect AKAP7δ/γ binding to PLB. Our attempts to measure the affinity of AKAP7γ for phosphorylated PLB (pPLB) by SPR indicate a complete lack of binding, which was supported in both transfected cells and stimulated rat neonatal myocytes. This finding is very interesting, and suggests that the AKAP7δ/γ-PLB interaction may be very dynamic. Given the phosphorylation dependence of this binding interaction, AKAP7γ may work by essentially shuttling PKA from one PLB molecule to the next as it binds, directs phosphorylation, and then unbinds to find its next unphosphorylated target. This sort of interaction has the potential to greatly amplify PLB phosphorylation.

To confirm whether the new finding of phosphorylation state binding dependency on PLB phosphorylation could in fact have such an amplification effect, we created an ordinary differential equation model of the complex dynamics. For AKAP-PLB interactions that are phosphorylation state-independent, the ability to achieve complete PLB phosphorylation would require at least an equimolar ratio of AKAP to PLB, since each PLB molecule would need an associated AKAP-PKA complex. In the range of AKAP concentrations tested, our model suggests that state-independent binding of AKAP to PLB cannot achieve levels of PLB phosphorylation that would allow for effective modulation of SERCA2a activity. Furthermore, the results suggested that state-independent binding would be insensitive to stimulation given that the dynamic range of phosphorylation with the maximum amount of AKAP tested is only ~0.2% of the total PLB concentration. However, state-dependent binding of AKAP to PLB enables small amounts of AKAP7γ to direct phosphorylation of much larger amounts of PLB. While the concentration of PLB is suggested to be 50μM or greater in cardiac myoctes, only 10–20% of the total PLB is in the monomeric form that can interact with and inhibit SERCA2a [2,14]. Our simulations show that at physiologically relevant concentrations of AKAP7δ/γ a dynamic range of PLB phosphorylation can be achieved such that complete phosphorylation of monomeric PLB is possible. Thus, phosphorylation state-specific binding could explain the ability of low abundance proteins such as AKAP7γ to regulate phosphorylation of high abundance proteins like PLB and troponin.

Data from our model also highlights the importance of the balance between AC and PDE activity, as well as PKA and phosphatase activity. The level of cAMP present in a given AKAP domain clearly defines the maximum dynamic range possible, as increased baseline cAMP results in higher baseline PKA activity resulting in a narrowed dynamic range of phosphorylation. While the increased baseline phosphorylation may be tempered by increased phosphatase activity, this too results in a slight decrease in the dynamic range of phosphorylation. Importantly, the significant increase in dynamic range seen with state-dependent binding, in comparison to state-independent binding, still exists with variation in baseline cAMP and phosphatase concentration.

This also raises a particularly intriguing hypothesis that such a mechanism may allow the cell to adapt to fluctuations in baseline cAMP concentration. As cAMP concentrations rise, additional phosphatase could restore baseline levels of phosphorylated substrate while still allowing for a great enough dynamic range to provide a detectable signal. This important role of phosphatase in the dynamic of PLB phosphorylation is consistent with several

published results demonstrating the importance of phosphatase inhibition for PLB phosphorylation, lending further credence to these findings [27–29].

6 Conclusions

Our findings reaffirm the importance of AKAP7 in directing phosphorylation of PLB and present a novel mechanism that can explain the decrease in PLB phosphorylation associated with human PLB mutants. The state-dependent binding of AKAP7δ/γ also explains how it may be possible that small quantities of AKAP and PKA could regulate phosphorylation of large amounts of substrate, as is the case for PLB and troponin. These findings require us to consider that AKAP complexes in general may be much more dynamic than previously thought. Further investigation of the AKAP7γ-PLB complex kinetics is warranted, as well as careful examination of other AKAP complexes that may also exhibit similar state-dependent interactions.

Supplementary Material

Refer to Web version on PubMed Central for supplementary material.

Acknowledgments

This work contains data from the doctoral thesis of Marc Rigatti (UCHC, Farmington, CT, USA).

Funding

This work was supported by an American Heart Association grant 12GRNT1216008 to K.L.D.-K. and a National Institutes of Health Grant P41-GM103313 to I.I.M.

Abbreviations

AKAP7	A-kinase anchoring protein
PLB	phospholamban
SERCA2a	Sarcoplasmic Reticulum Ca^{2+}-ATPase
PKA	Protein Kinase A
GFP	green fluorescent protein
SPR	surface plasmon resonance

References

1. Kapiloff MS, Rigatti M, Dodge-Kafka KL. J. Gen. Physiol. 2014; 143:9–15. [PubMed: 24378903]
2. MacLennan DH, Kranias EG. Nat Rev Mol Cell Biol. 2003; 4:566–577. [PubMed: 12838339]
3. Lygren B, Carlson CR, Santamaria K, Lissandron V, McSorley T, Litzenberg J, Lorenz D, Wiesner B, Rosenthal W, Zaccolo M, Taskén K, Klussmann E. EMBO Rep. 2007; 8:1061–1067. [PubMed: 17901878]
4. Carnegie GK, Means CK, Scott JD. IUBMB Life. 2009; 61:394–406. [PubMed: 19319965]
5. Fink MA, Zakhary DR, Mackey JA, Desnoyer RW, Apperson-Hansen C, Damron DS, Bond M. Circulation Research. 2001; 88:291–297. [PubMed: 11179196]

6. Patel HH, Hamuro LL, Chun BJ, Kawaraguchi Y, Quick A, Rebolledo B, Pennypacker J, Thurston J, Rodriguez-Pinto N, Self C, Olson G, Insel PA, Giles WR, Taylor SS, Roth DM. Journal of Biological Chemistry. 2010; 285:27632–27640. [PubMed: 20581396]
7. Kritzer MD, Li J, Dodge-Kafka K, Kapiloff MS. Journal of Molecular and Cellular Cardiology. 2012; 52:351–358. [PubMed: 21600214]
8. Trotter KW, Fraser I, Scott GK, Stutts MJ. The Journal of Cell …. 1999
9. Johnson KR, Nicodemus-Johnson J, Carnegie GK, Danziger RS. BMC Evolutionary Biology. 2012; 12:125. [PubMed: 22834419]
10. Lygren B, Taskén K. Expert Opin. Biol. Ther. 2008; 8:1099. [PubMed: 18613762]
11. Cantrell AR, Tibbs VC, Yu FH, Murphy BJ, Sharp EM, Qu Y, Catterall WA, Scheuer T. Mol. Cell. Neurosci. 2002; 21:63. [PubMed: 12359152]
12. Singh A, Redden JM, Kapiloff MS. Molecular Pharmacology. 2011; 79:533–540. [PubMed: 21149637]
13. Ahmad F, Shen W, Vandeput F. Journal of Biological …. 2015
14. Bers DM. Nature. 2002; 415:198. [PubMed: 11805843]
15. Saucerman JJ, McCulloch AD. Prog. Biophys. Mol. Biol. 2004; 85:261. [PubMed: 15142747]
16. Saucerman JJ, Brunton LL, Michailova AP, McCulloch AD. Journal of Biological Chemistry. 2003; 278:47997. [PubMed: 12972422]
17. Redden MJ, Le AV, Singh a, Federkiewicz K, Smith S, Dodge-Kafka KL. Biochemical J. 2012; 446:301–309.
18. Scholten A, van Veen TA, Vos AMA, Heck AJ. Journal of Proteome Research. 2007; 6:1705–1717. [PubMed: 17432891]
19. Jones BW, Brunet S, Gilbert ML, Nichols CB, Su T, Westenbroek RE, Scott JD, Catterall WA, McKnight GS. Proc. Natl. Acad. Sci. U.S.a. 2012; 109:17099. [PubMed: 23035250]
20. Kapiloff MS, Schillace RV, Westphal AM, Scott JD. J Cell Sci. 1999; 112:2725. [PubMed: 10413680]
21. Dodge-Kafka KL, Soughayer J, Pare GC, Michel JJC, Langeberg LK, Kapiloff MS, Scott JD. Nature. 2005; 437:574–578. [PubMed: 16177794]
22. Alto NM, Soderling SH, Hoshi N, Langeberg LK, Fayos R, Jennings PA, Scott JD. Proc. Natl. Acad. Sci. U.S.a. 2003; 100:4445. [PubMed: 12672969]
23. Gold MG, Stengel F, Nygren PJ, Weisbrod CR, Bruce JE, Robinson CV, Barford D, Scott JD. Proc. Natl. Acad. Sci. U.S.a. 2011; 108:6426. [PubMed: 21464287]
24. Schmitt JP. Science. 2003; 299:1410. [PubMed: 12610310]
25. Haghighi K, Kolokathis F, Pater L, Lynch RA, Asahi M, Gramolini AO, Fan G-C, Tsiapras D, Hahn HS, Adamopoulos S, Liggett SB, Dorn II GW, MacLennan DH, Kremastinos DT, Kranias EG. J. Clin. Invest. 2003; 111:869. [PubMed: 12639993]
26. Weisenhaus M, Allen ML, Yang L, Lu Y, Nichols CB, Su T, Hell JW, McKnight GS. PLoS ONE. 2010; 5:e10325. [PubMed: 20428246]
27. Kranias EG. Journal of Biological Chemistry. 1985; 260:11006. [PubMed: 2993298]
28. Nicolaou P, Rodriguez P, Ren X, Zhou X, Qian J, Sadayappan S, Mitton B, Pathak A, Robbins J, Hajjar RJ, Jones K, Kranias EG. Circulation Research. 2009; 104:1012. [PubMed: 19299645]
29. Pathak A, del Monte F, Zhao W, Schultz J-E, Lorenz JN, Bodi I, Weiser D, Hahn H, Carr AN, Syed F, Mavila N, Jha L, Qian J, Marreez Y, Chen G, McGraw DW, Heist EK, Guerrero JL, DePaoli-Roach AA, Hajjar RJ, Kranias EG. Circulation Research. 2005; 96:756. [PubMed: 15746443]

Highlights

- AKAP7δ/γ link PKA to phospholamban, enhancing phosphorylation of Phospholabman
- This interaction is disrupted in several defined human mutations
- Phosphorylation of phospholamban significantly decreases the affinity for AKAP7δ/γ, allowing for state-dependent binding of the AKAP
- Computational analysis of this signaling pathway suggests that state-dependent binding allows for small concentrations of AKAP7δ/γ and PKA to phosphorylated the large quantities of phospholamban seen in the cardiac myocyte

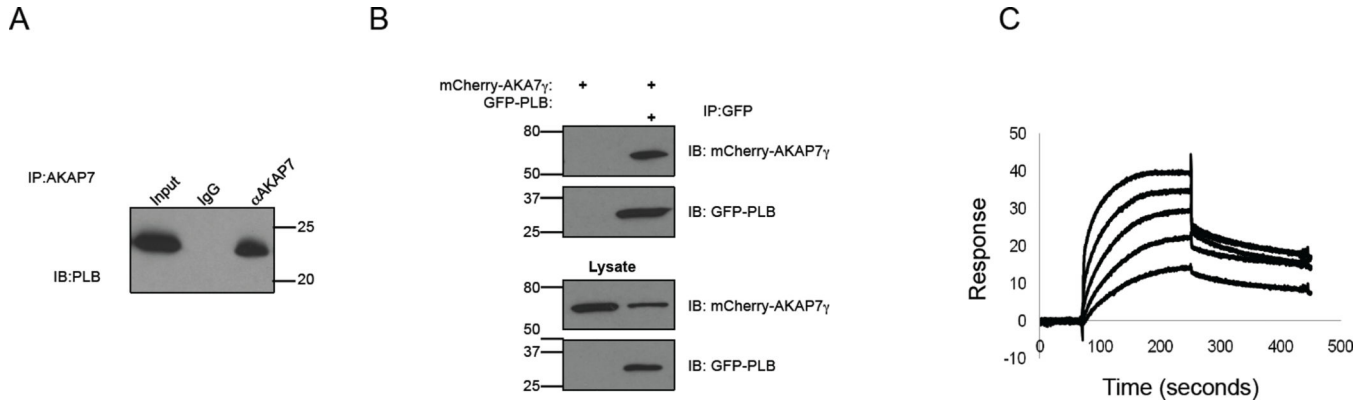

Figure 1. Direct cellular interaction between AKAP7δ/γ and phospholamban

A) AKAP7 was immunoprecipitated from rat heart extract and association of PLB was determined by Western Blot. n=3. **B)** mCherry Western blot analysis of anti-GFP immunoprecipitates isolated from HEK-293 cells co-transfected with mCherry-AKAP7γ in the presence and absences of GFP-PLB (upper panels). To confirm immunoprecipitation of equal amounts of GFP-PLB, the nitrocellulose membranes were also probed for GFP using a monoclonal anti-GFP antibody (middle panel). Lower panels depict mCherry and GFP Western blot analysis of the input (20 μL) from each condition. n=3. **C)** SPR was performed by immobilizing a peptide containing the first 21 amino acids of PLB (150RUs) on a CM-5 chip and measuring the response when passing over a range of concentrations (12.5–200nM) of AKAP7γ. Forward and reverse rates of binding and binding affinity were determined by fitting of the sensorgram with BIAcore T100 evaluation software.

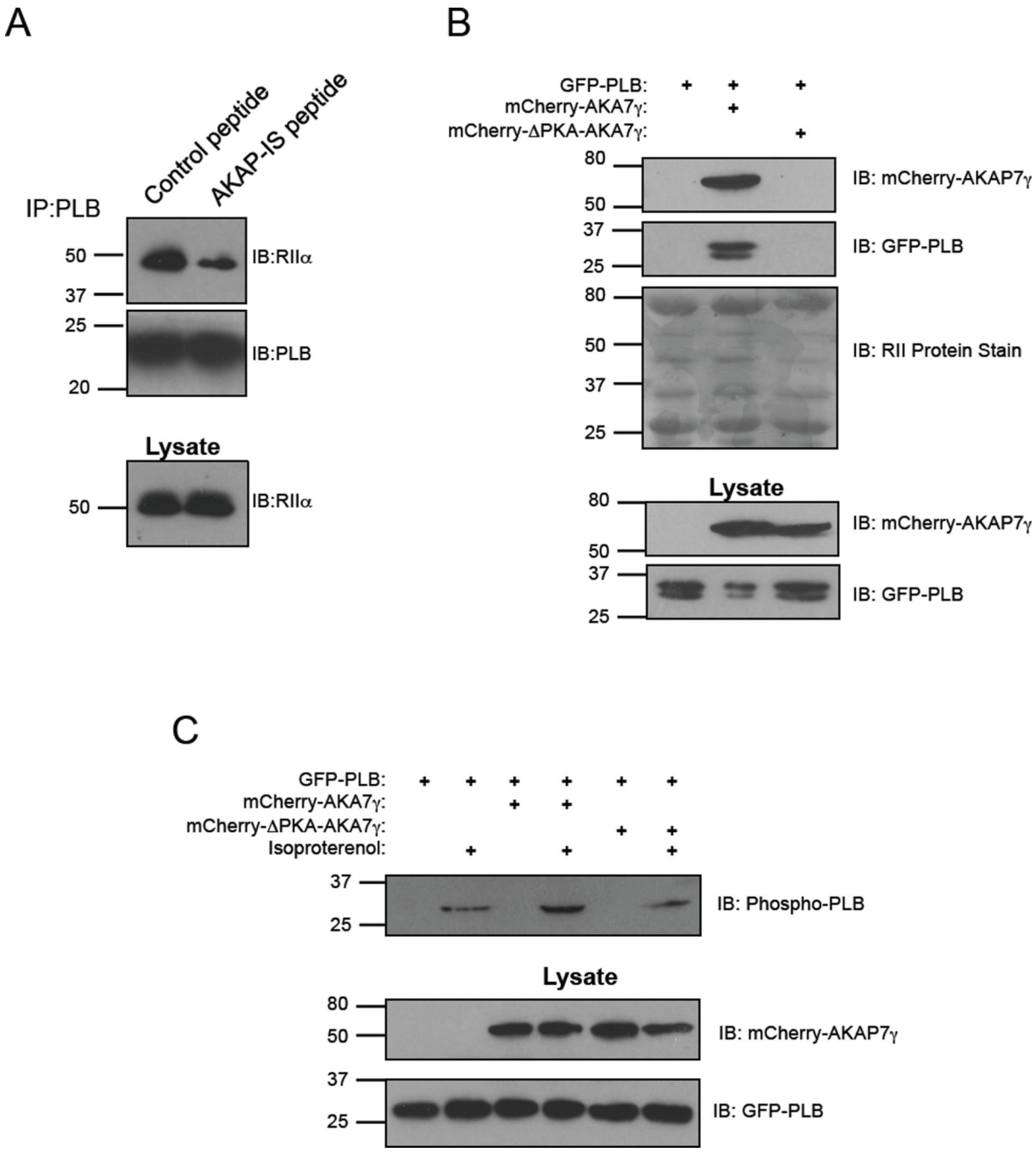

Figure 2. AKAP7δ/γ anchors PKA to the phospholamban complex to enhance phosphorylation

A) PLB was immunoprecipitated from rat heart lysate. Following extensive washing, the immunoprecipitates were incubated with the AKAP/PKA disrupting peptide AKAP-IS (10 μM) or control peptide (10 μM) for 30 minutes while rocking. After another round of washing, association of the regulatory subunit of PKA was determined by Western blot. **B**) HEK-293 were transfected with GFP-PLB and either wild-type mCherry-AKAP7γ, or one deficient in the PKA binding domain (mCherry-ΔPKA-AKAP7γ). Isolated lysates were subjected to pulldown assays using bacterially purified GST-tagged PKA RII subunit

precharged on Glutatione-agarose; Both GFP and mCherry antibodies were used for detecting PLB and AKAP7γ interactions, respectively (upper panel). Protein stain of the nitrocellulose membrane before Western blot analysis is shown in the middle panel. Input from the transfected cells (20μl) is shown in the bottom panels. n=3. **C)** HEK-293 were transfected with GFP-PLB and either wild-type mCherry-AKAP7γ, or one deficient in the PKA binding domain (mCherry-ΔPKA-AKAP7γ). Cells were stimulated with 100 μM Isoproterenol for 5 minutes before cell lystate was isolated and loaded onto and SDS-PAGE gel. Phosphorylation of PLB at Serine 16 was determined using a phospho-specific antibody (upper panel). Total expression of the proteins is shown in the lower panels using both GFP and mCherry antibodies to detect PLB and AKAP7γ, respectively. n=3

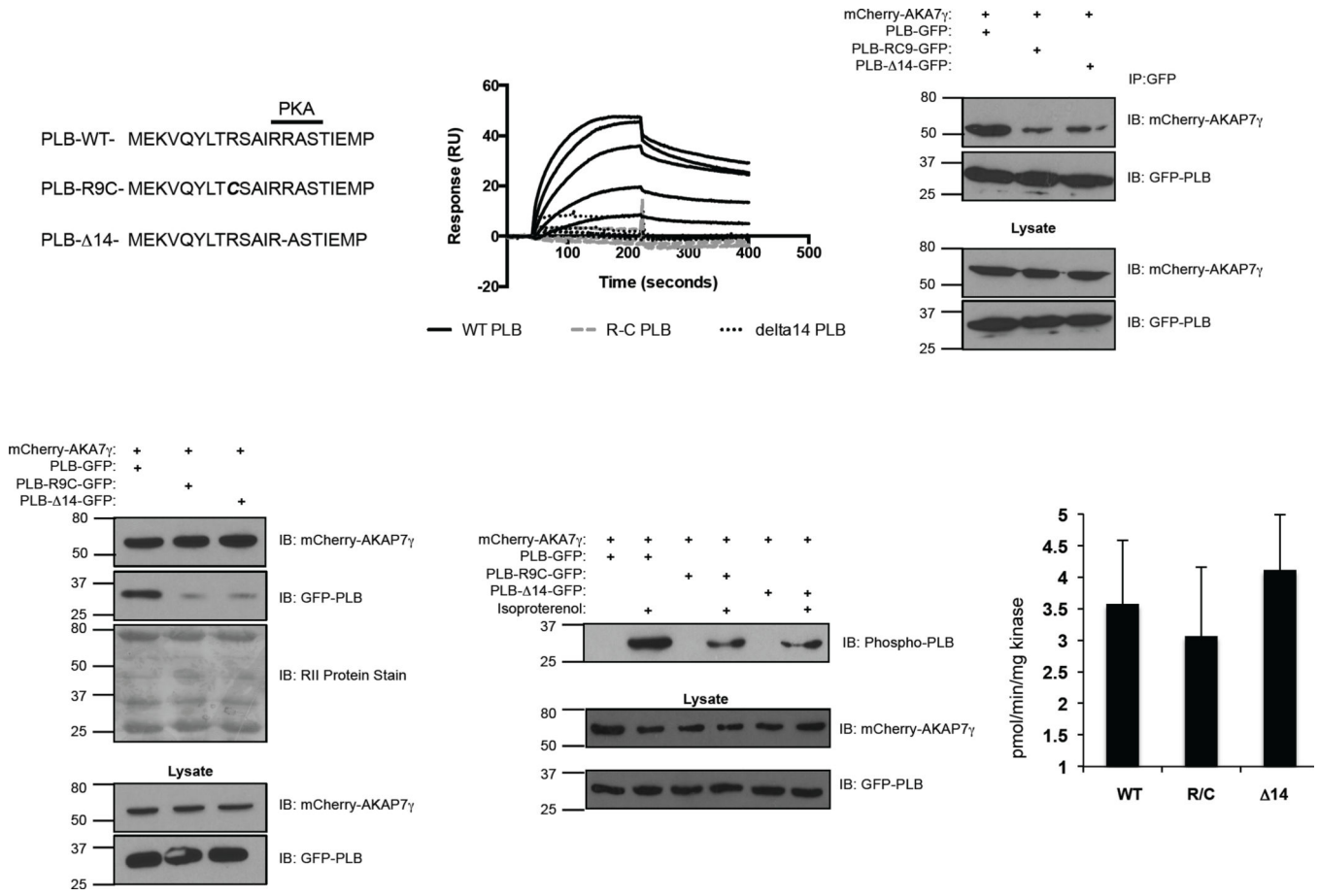

Figure 3. Described human mutations of phospholamban disrupt AKAP7γ binding

Schematic depiction of the mutations found in phospholamban that are found in the AKAP7δ/γ binding domain. **B)** SPR was performed by immobilizing a peptide containing the first 21 amino acids of either wild-type PLB, or one containing either the R9C or the Δ14 mutation (150RUs) on a CM-5 chip and measuring the response when passing over a range of concentrations (12.5–200nM) of AKAP7γ. The binding affinity between the two proteins was determined by the BIAcore T100 evaluation software. **C)** mCherry Western blot analysis of anti-GFP immunoprecipitates isolated from HEK-293 cells co-transfected with mCherry-AKAP7γ and either wild-type GFP-PLB, or one of the mutated isoforms (PLB-RC9-GFP, or PLB-Δ14-GFP, upper panels). To confirm immunoprecipitation of equal amounts of GFP-PLB, the nitrocellulose membrane was also probed for GFP using a monoclonal anti-GFP antibody (middle panel). Lower panels depict mCherry and GFP Western blot analysis of the input (20 μL) from each condition. n=3. **D)** HEK-293 were transfected with mCherry-AKAP7γ and either wild-type GFP-PLB, or one of the mutated isoforms (PLB-RC9-GFP, or PLB-Δ14-GFP, upper panels). Isolated lysates were subjected to pulldown assays using bacterially purified GST-tagged PKA RII subunit precharged on Glutatione-agarose; Both GFP and mCherry antibodies were used for detecting PLB and AKAP7γ interactions, respectively (upper panel). Protein stain of the nitrocellulose membrane before Western blot analysis is shown in the middle panel. Input from the transfected cells (20μl) is shown in the bottom panels. n=3. **E)** HEK-293 were transfected

with mCherry-AKAP7γ and either wild-type GFP-PLB, or one of the mutated isoforms (PLB-RC9-GFP, or PLB-Δ14-GFP. Cells were stimulated with 100 μM Isoproterenol for 5 minutes before cell lystate was isolated and loaded onto and SDS-PAGE gel. Phosphorylation of PLB at Serine 16 was determined using a phospho-specific antibody (upper panel). Total expression of the proteins is shown in the lower panels using both GFP and mCherry antibodies to detect PLB and AKAP7γ, respectively. n=3 E) PLB peptides (1 μg) were incubated in kinase buffer (50 mM Tris-HCL pH 7.5, 5 mM $MgCl_2$) containing 100 μM ATP, 5 μM [γ^{-32}]ATP and 800 units of purified PKA catalytic subunit (NEB). After a 15 minute incubation at 30°C, the reaction mixture was spotted onto phosphocellulose strips and washed five times in 75 mM phosphoric acid. Filters were air dried and counted.

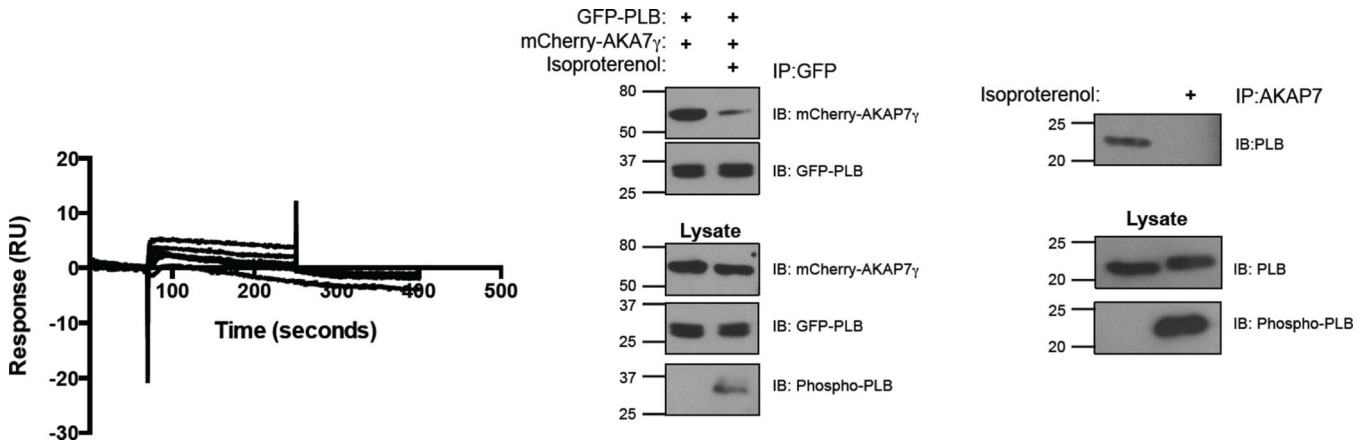

Figure 4. Phosphorylation of PLB significantly decreases the affinity for AKAP7δ/γ

A) SPR was performed by immobilizing a peptide containing the first 21 amino acids of PLB that had been phosphorylated (150RUs) on a CM-5 chip and measuring the response when passing over a range of concentrations (12.5–200nM) of AKAP7γ. The binding affinity between the two proteins was determined by the BIAcore T100 evaluation software. **B)** HEK-293 were transfected with GFP-PLB and mCherry-AKAP7γ. Cells were stimulated with 100 μM Isoproterenol for 5 minutes and the PLB complex was isolated by immunoprecipitation using anti-GFP. Association of AKAP7γ was determined by Western blot using anti-mCherry (upper panels). To confirm immunoprecipitation of equal amounts of GFP-PLB, the nitrocellulose membrane was also probed for GFP using a monoclonal anti-GFP antibody (middle panel). Total expression of the proteins is shown in the lower panels using both GFP and mCherry antibodies to detect PLB and AKAP7γ, respectively. Phosphorylation of PLB at Serine 16 in total lysate was determined using a phospho-specific antibody (upper panel). n=3 C) Rat neonatal cardiac myocytes were stimulated with 10 μM Isoproterenol for 5 minutes and the PLB complex was isolated by immunoprecipitation. Association of AKAP7δ/γ was determined by Western blot (upper panel). Total expression of the proteins is shown in the lower panels. Phosphorylation of PLB at Serine 16 in total lysate was determined using a phospho-specific antibody (upper panel). n=3

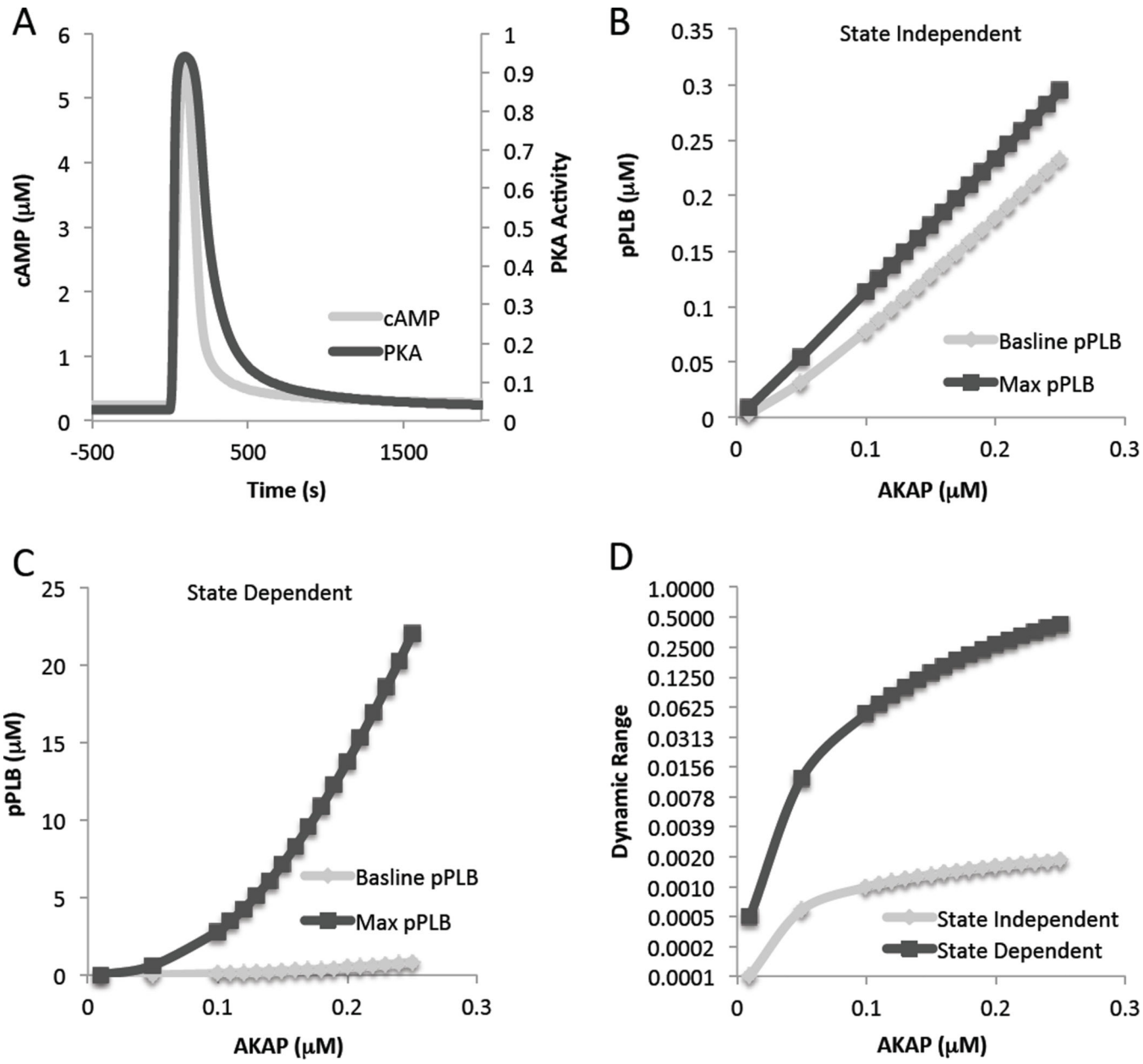

Figure 5. State dependent binding of AKAP to PLB dramatically increases PLB phosphorylation upon stimulation

A) cAMP concentration and PKA activity over the time-course of the simulations. All species in the model are at steady state prior to stimulation (t = 0s), which was achieved via activation of additional AC. **B)** pPLB concentration at baseline and maximum following stimulation for state independent binding of AKAP and PLB. C) pPLB concentration at baseline and maximum following stimulation for state dependent binding of AKAP and PLB. D) Dynamic range $(Dynamic\ Range = \frac{(Max\ pPLB - Min\ pPLB)}{Total\ PLB})$ of PLB phosphorylation for both state dependent and state independent binding of AKAP to PLB. The y-axis is on a $\log_2$ scale to enable viewing of both trends on the same graph.

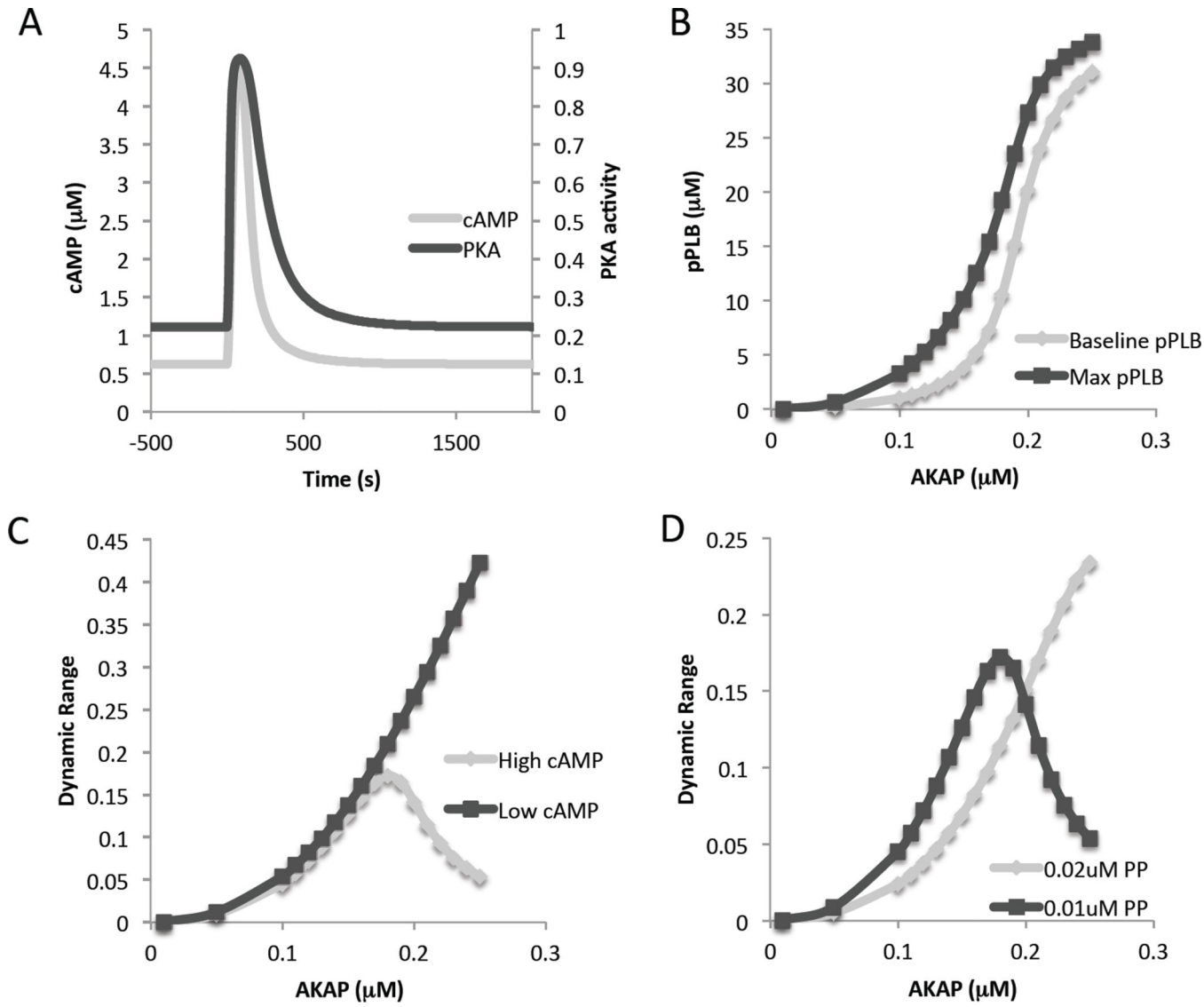

Figure 6. Increased baseline cAMP reduces dynamic range of PLB phosphorylation

A) cAMP concentration and PKA activity over the time-course of the simulations as in figure 5. The concentrations of AC and PDE have been adjusted to increase the baseline level of cAMP from 244nm to 622nm. **B)** pPLB concentration at baseline and maximum following stimulation for state dependent binding of AKAP and PLB. **C)** Dynamic range of PLB phosphorylation for state dependent phosphorylation at low (244nM) and high (622nM) baseline cAMP levels given AKAP concentrations ranging from 1nM to 250nM. **D)** Dynamic range of PLB phosphorylation with high baseline levels of cAMP and normal or increased protein phosphatase (PP).